Surface Properties of Ni−Pt/SiO_2 Catalysts for N_2O Decomposition and Reduction by H_2†

Jesús Arenas-Alatorre,‡ Antonio Gómez-Cortés,‡ Miguel Avalos-Borja,§ and Gabriela Díaz*,‡

Instituto de Física-UNAM, Apdo. Postal 20-364, C.P. 01000, México, D.F. and Centro de Ciencias de la Materia Condensada-UNAM, Apdo Postal 2681 C.P. 22800, Ensenada, B.C. México

Received: March 15, 2004; In Final Form: June 21, 2004

The surface properties of bimetallic Ni−Pt/SiO_2 catalysts with variable Ni/Ni + Pt atomic ratio (0.75, 0.50, and 0.25) were studied using N_2O decomposition and N_2O reduction by hydrogen reactions as probes. Catalysts were prepared by incipient wetness impregnation of the silica support with aqueous solutions of the metal precursors to a total metal loading of 2 wt %. For both model reactions, Pt/SiO_2 catalyst was substantially more active than Ni/SiO_2 catalyst. Mean particle size by TEM was about the same (in the range 6−8 nm) for all catalysts and truly bimetallic particles (more than 95%) were evidenced by EDS in the Ni−Pt/SiO_2 catalysts. CO adsorption on the bimetallic catalysts showed differences in the linear CO absorption band as a function of the Ni/Pt atomic ratio. Bimetallic Ni−Pt/SiO_2 catalysts showed, for the N_2O decomposition, a catalytic behavior that points out an ensemble-size sensitive behavior for Ni-rich compositions. For the $N_2O + H_2$ reaction, the bimetallic catalysts were very active at low temperature. The following activity order at 300 K was observed: $Ni_{75}Pt_{25} > Ni_{25}Pt_{75} \approx Ni_{50}Pt_{50} >$ Pt. TOF values for these catalysts increased 2−5 times compared to the most active reference catalyst (Pt/SiO_2). The enhancement of the activity in the $Ni_{75}Pt_{25}$ bimetallic catalysts is explained in terms of the presence of mixed Ni−Pt ensembles.

Introduction

Bimetallic catalysts often present superior performance compared to monometallic catalysts. The changes that occur at the surface due to alloying may be reflected by changes in the selectivity, activity, and/or stability of the catalyst.[1] The catalytic properties of bimetallic catalysts usually deviate from additive properties of the metal components. Two models have been proposed to explain such a result:[2] (i) the ensemble effect that is geometric in nature, in which the second metal may block sites on the surface of the active metal, and, by that the average size and composition of the ensembles of active sites is varied, and (ii) the electronic effect in which unexpected catalytic properties are the result of the modification of the electronic environment of the active phase due to alloying. The characterization of the phases present in bimetallic systems is consequently of great importance in any attempt to understand the behavior of a bimetallic catalyst.

In particular, the Ni−Pt system is an interesting bimetallic system as reviewed by Ponec and Bond.[3] This system in the form of single-crystal bulk alloys, thin films, and supported catalysts has attracted the attention of many groups for many years.[4−15] Characterization studies on Pt−Ni alloy single-crystal surfaces have shown a unique orientation dependence of surface segregation as well as surface reconstruction phenomena.[6−13]

Platinum and nickel exhibit different catalytic and reducibility properties. These metals are active in a great number of reactions of practical importance, such as hydrogenation, isomerization, and reforming. The addition of Ni to Pt catalysts (near to the 1:1 atomic ratio) has been reported to increase the activity and selectivity in the gas-phase hydrogenation of crotonaldehyde[16] and acetonitrile,[17] and to exhibit mechanism changes toward hydrocarbon isomerization.[18] On the other hand, Massardier et al.[19] have shown for $Pt_{78}Ni_{22}$(111) and $Pt_{50}Ni_{50}$(111) alloys quite different chemisorptive properties; while in the former the adsorption of benzene and ethane is similar to that on pure Pt(111), in the latter chemisorption of these molecules is very weak, even thought platinum segregation forms a quasi-pure platinum layer. Bertolini[13] explained the influence of strain in the electronic properties of the surface atoms as the most probable reason for the modification of the chemical reactivity of PtNi alloys.

In previous research, HREM microstructural characterization of $Ni_{50}Pt_{50}/SiO_2$ catalysts using electron microscopy techniques was performed to obtain knowledge on the microstructure of the metallic nanophases.[21] The formation of truly bimetallic particles with various metal compositions was evidenced. Among these, the Ni/Pt = 3 and Ni/Pt = 1 compositions were predominant. Nanoparticles of the Ni_3Pt and NiPt intermetallic phases were identified by HREM. In this work, we extended the research to the evaluation of the catalytic performance and characterization of a series of Ni−Pt/SiO_2 catalysts with various metal compositions. The goal was to examine the influence of the catalyst composition in the catalytic properties using as model reactions the nitrous oxide decomposition and reduction by hydrogen. The interaction of N_2O with metal surfaces is an interesting topic in catalysis since nitrous oxide has been identified, on one hand, as a greenhouse gas[22] and, on the other, as an intermediate in the removal process of nitric oxides.[23] The catalytic decomposition of N_2O on supported metals and oxides has been the subject of many works as can be seen in the review of Kapteij et al.[24] On the other hand, several investigations on adsorption and decomposition of N_2O on well-defined fcc surfaces have shown that (111) surfaces such as Pt(111)[25] are inert toward N_2O dissociation; whereas, other

† Part of the special issue "Michel Boudart Festschrift".

* Corresponding Author: Dr. Gabriela Diaz. Instituto de Física UNAM, Apdo. Postal 20-364, C. P. 01000, México, D. F. Phone: +(5255)56225097. Fax: +(5255)56225008. E-mail: diaz@fisica.unam.mx.

‡ Instituto de Física-UNAM.

§ Centro de Ciencias de la Materia Condensada-UNAM.

10.1021/jp048843q CCC: $30.25
Published on Web 08/11/2004

planes are active, such as Ni (100),[26] Ni(110),[27] Ni (755),[28] polycrystalline surfaces of Pt,[29] and supported Pt.[30] Although interaction of N_2O has been studied on Pt and Ni surfaces, we could find no studies related to this topic on Ni−Pt surfaces.

Experimental Section

(a) Catalyst Preparation. The catalysts, Pt, Ni, and bimetallic Ni−Pt, were prepared by incipient wetness impregnation of SiO_2 (Degussa, S = 200 m^2/g), hereafter noted as S200, using an aqueous solution containing the desired concentration of $H_2PtCl_6 \cdot 6H_2O$ (Merck) or $Ni(NO_3)_2$ (Aldrich) used as metallic precursors. The total metal loading was 2 wt % and the atomic composition of the bimetallic catalysts was fixed at Ni/Ni + Pt = 0.75, 0.50, and 0.25. Coimpregnation of the support was used in the case of bimetallic samples. After drying at 373 K, the Ni and bimetallic samples were calcined in flowing air at 673 K for 2 h and then reduced in pure H_2 at 873 K for the same period of time. The monometallic Pt catalyst, after drying at 373 K, was reduced in H_2 at 773 K for 2 h without prior calcination. For catalysts in plots, the notation is M/S200 where M = Pt, Ni, or Ni_xPt_y (x, y denotes the nominal atomic percentage of each metal in the bimetallic catalyst).

(b) Characterization Techniques. Electron Microscopy. Mean particle size (d_s) and particle size distribution were obtained from conventional transmission electron microscopy by means of a JEOL 2010 F electron microscope. On the other hand, a characterization of the catalyst microstructure was achieved using a JEOL 4000EX high-resolution electron microscope (resolution ∼1.7 Å). Image processing and image simulation (multislice method) techniques were also applied. Additionally, EDS microanalysis (NORAN, model Voyager 4.2.3) for elemental chemical analysis on particles of 3.0 nm and larger was used to check the chemical composition of the metallic particles. For TEM, EDS, or HREM analysis, samples were crushed in an agate mortar and the powder was suspended in isopropyl alcohol. A drop was placed on commercial holey carbon copper grids. The electron microscopes were calibrated using a gold thin film.

Thermo-programmed Reduction (TPR). Experiments were done in a multitask characterization unit RIG-100 from In Situ Research Experiments Inc. The calcined sample was placed in the quartz reactor, purged with Ar at room temperature, and then heated at a rate of 10 K/min in the presence of a 5% H_2/Ar gas mixture (30 mL/ min) to reach 873 K.

FTIR Spectroscopy. CO adsorption was used to characterize the surface of the catalysts. Diffuse reflectance infrared Fourier transformed spectra (DRIFT) were collected using a Nicolet Portegé P-450 FTIR spectrometer with a resolution of 4 cm^{-1}, equipped with a high-temperature environmentally controlled cell (Spectra Tech). About 0.020 g of powdered sample was packed in the sample holder and pretreated in situ in the DRIFT cell under H_2 flow at 673 K and kept for 1h. After this treatment, the sample was purged with He (30 min) and cooled to room temperature in the same gas atmosphere. The CO (1% CO/He) was then allowed to flow over the catalyst (20 min). Afterward, helium was admitted in the system. Spectra were collected from 512 scans and in all cases difference spectra were obtained by making reference to the freshly reduced solid prior to CO adsorption. The bands of any residual CO gas phase were also removed from the spectra using appropriate subtraction procedures. The spectrum of dry KBr was taken for IR single-beam background subtraction.

Catalytic Activity. The reactivity of the catalysts was studied using N_2O as a probe. Two reactions were considered, the catalytic decomposition of N_2O and the reduction of N_2O by hydrogen. Both reactions were studied in the temperature range 300−973 K using a commercial flow system (RIG-100) working at atmospheric pressure. The reactant concentration (H_2 and/or N_2O) was 2500 ppm (balance He) and the N_2O/H_2 molar ratio for the $N_2O + H_2$ reaction was 1. The samples (typically 0.1 g) were reactivated in H_2 at 673 K for 1 h prior to the catalytic runs. The reactant mixture (GHSV = 25 000 h^{-1}) was fed to the microreactor at room temperature after the system was purged in He. The reactor temperature was then increased and catalytic activity was evaluated. For each increment of temperature, enough time was given to allow the conversion of N_2O to stabilize. Total activity was followed by the N_2O consumption as a function of the reaction temperature according to % $\alpha_{N_2O} = [[N_2O]_{in} - [N_2O]_{out}/[N_2O]_{in}](100)$, where $[N_2O]_{in}$ and $[N_2O]_{out}$ are the N_2O concentration at the inlet and at the exit of the reactor, respectively. The reaction products were analyzed by gas chromatography using a 4-m packed Chromosorb 103 column. Calibration for quantitative analysis was performed using pure gases. Estimated error in activity data is in the range ±2%. A steady-state N_2O reduction rate was calculated as $-r_{N_2O} = \alpha F/\omega$, where α is the N_2O conversion as previously defined, F is the flow rate of N_2O (mol/s), and ω is the weight of the catalyst (g).

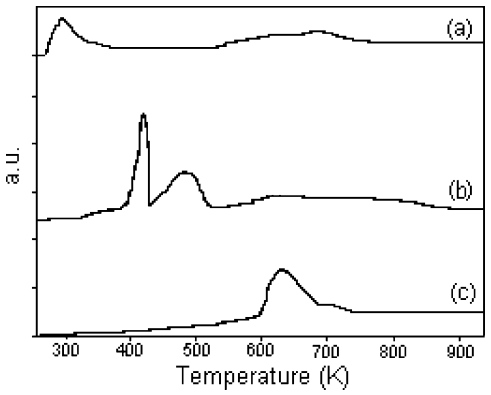

Figure 1. TPR profiles of Ni−Pt/SiO_2 samples calcined at 673 K: (a) Pt/SiO_2, (b) $Ni_{50}Pt_{50}$/S200, and (c) Ni/SiO_2.

Results and Discussion

TPR experiments provided information about the reduction temperatures of the oxide phases. Figure 1 presents the comparison between the TPR profiles of Pt/SiO_2 and Ni/SiO_2 and the bimetallic $Ni_{50}Pt_{50}$/S200 catalyst. The calcined nickel sample presented a broad reduction peak at 670 K. Reduction of the Pt oxide phase took place at significantly lower temperature (around 300 K). When a calcined bimetallic catalyst is submitted to a thermoprogrammed reduction, the TPR profile showed two main reduction peaks attributed to reduction of Pt and Ni oxide phases. A significant feature was that the reduction peak attributed to reduction of Ni is shifted to lower temperatures (523 K) compared to the monometallic Ni catalyst. The presence of platinum in the bimetallic catalyst seems to facilitate the reduction of nickel atoms. The driving force for this phenomenon is the easier availability of hydrogen (dissociation and spillover) in the presence of the noble metal. Collective effects such as this have been reported for several bimetallic systems. A detailed work from Jentys et al.[31] about the reduction kinetics during TPR experiments of silica-supported bimetallic Pt−Ni catalysts prepared from chloride precursors with various metal compositions, studied by XANES, has shown that for Ni-rich catalysts, the final reduction of the catalyst occurred in two

TABLE 1: Particle Size (d_s) Determined by TEM

catalyst M/S200	d_s (nm)
Pt	7.5
$Ni_{25}Pt_{75}$	5.8
$Ni_{50}Pt_{50}$	7.6
$Ni_{75}Pt_{25}$	7.0
Ni	6.9

M = Pt, Ni, or Ni−Pt. S200 = SiO_2 Degussa.

TABLE 2: Percentage of Particles Showing Single or Bimetallic Compositions as Determined by EDS Analysis

catalyst	Pt	Ni−Pt	Ni
$Ni_{75}Pt_{25}$	-	96	4
$Ni_{50}Pt_{50}$	5	95	-
$Ni_{25}Pt_{75}$	2	98	-

steps. In the first, the reduction of adjacent Pt atoms and Ni atoms took place, forming a bimetallic phase; in the second, reduction of the remaining Ni atoms occurred, forming a separate Ni phase. These results showed that the presence of Pt lowered the reduction temperature of Ni.

Particle size (d_s) determined by TEM was about the same for all catalysts (Table 1). Pt/SiO_2 presented the highest value (7.5 nm) and the $Ni_{75}Pt_{25}$ bimetallic sample the lowest (5.8 nm). TEM and HREM images showed significant differences in the shape and crystalline lattice of the Pt and Ni particles in the monometallic samples taken as reference. Opposite to particle morphologies observed in the Pt/SiO_2 catalysts, the nickel particles in the Ni/SiO_2 catalysts presented irregular morphologies with a tendency to wet the support. While in the Pt/SiO_2 catalyst, only reduced Pt particles were identified, in the Ni/SiO_2 sample some lattice measurements showed the presence of the NiO phase.[21] EDS analysis, on a particle-by-particle basis, showed (in the three bimetallic samples) the simultaneous presence of Ni and Pt atoms in the particles. Quantitative analysis revealed (Table 2) that in these catalysts more than 95% of the analyzed particles were bimetallic. Metal composition in the particles ranged from Ni-rich to Pt-rich, but in all three bimetallic catalysts the predominant compositions in the particles were the nominal and the $Ni_{50}Pt_{50}$ composition. As seen from Table 2, a small percentage of Pt-only particles was detected in the Pt rich catalysts and Ni-only particles were observed in the $Ni_{75}Pt_{25}$ catalyst. HREM characterization of the structure of $Ni_{50}Pt_{50}$ catalyst showed[21] that particles, mostly with defects as single twinning, multiple twinning (MTP), and stacking faults, were present. The crystallographic orientation of these particles was predominantly [011] with cubooctahedral shapes. Superlattice structures were also identified and confirmed by image simulation. The characterization of the microstructure allowed us to identify the Ni_3Pt and NiPt intermetallic phases among the bimetallic phases detected by EDS. Already, in an EXAFS analysis performed during temperature-programmed reduction of silica supported platinum and nickel chlorides,[32] it was shown that a bimetallic phase is formed during the reduction of the catalyst precursors, and that as a function of the catalyst composition, the reduced catalyst consisted of at least one bimetallic phase (NiPt) and the pure phase of the metal which remained unalloyed. For catalysts with more than 50 at. % Ni, the authors concluded that there was either an enrichment of the bimetallic phase in Ni or the formation of a second bimetallic phase (Ni_3Pt). Figure 2 shows a typical HREM image of $Ni_{75}Pt_{25}$/S200 catalyst.

The N_2O decomposition and reduction by hydrogen was used to characterize the surface reactivity of the solids. Figure 3 shows the overall N_2O conversion as a function of the reaction

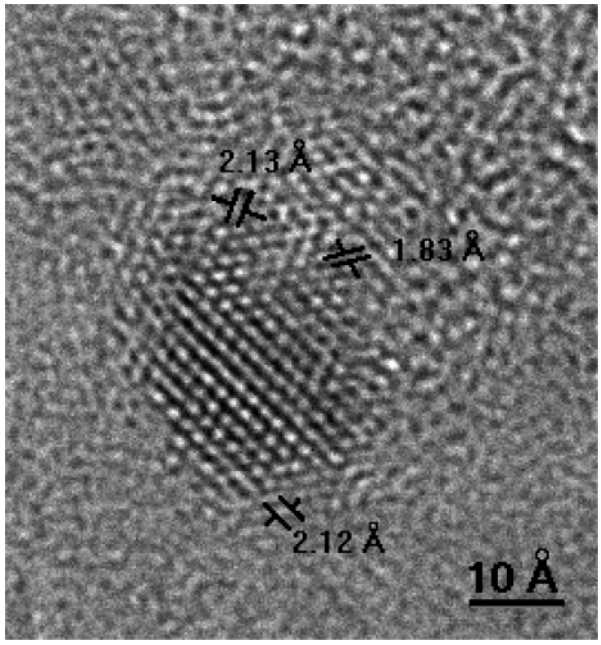

Figure 2. HREM image of a bimetallic particle in $Ni_{75}Pt_{25}$/S200.

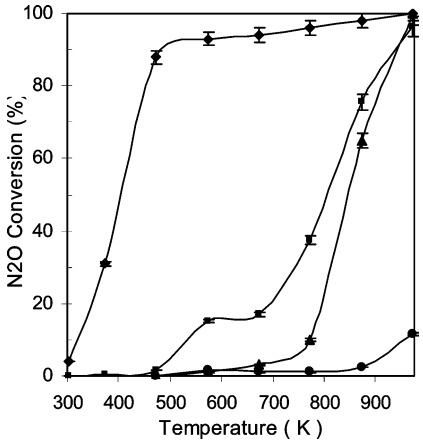

Figure 3. Catalytic performance of Ni and Pt monometallic catalysts. Evolution of the N_2O conversion as a function of the reaction temperature for N_2O decomposition (D−M/SiO_2) and N_2O reduction by H_2 (R−M/SiO_2): ■, R−Ni/SiO_2; ◆, R−Pt/S200; ●, D−Ni/S200; and ▲, D−Pt/S200.

temperature displayed by monometallic Ni and Pt catalysts, for N_2O decomposition (D−M/S200) and for its reduction by hydrogen (R−M/S200). The activity of the Ni/SiO_2 catalyst for the N_2O decomposition is very low, less than 10% conversion at 973 K. On the contrary, on Pt/SiO_2 catalyst, 50% of the N_2O has been transformed at 825 K and total conversion is achieved at 973 K. The addition of hydrogen to the reactant mixture has a pronounced effect on the reactivity of the catalysts. A significant improvement of the catalytic reactivity of the samples is observed, the Ni/SiO_2 catalyst showed 50% N_2O conversion at 800 K and practically all the N_2O is transformed at 973 K. In the case of Pt/SiO_2 catalyst, 50% N_2O conversion is achieved at 380 K and about 90% of the reactant is already transformed at 450 K.

The differences in catalytic behavior for the transformation of N_2O of the set of catalysts are explained in terms of the reaction mechanism.[24] The N_2O decomposition can be described by the following steps: (a) the adsorption of N_2O at an active site on the surface, (b) decomposition of the adsorbed molecule with N_2 formation to leave surface oxygen, and (c) this surface oxygen desorbs by combination with another surface oxygen

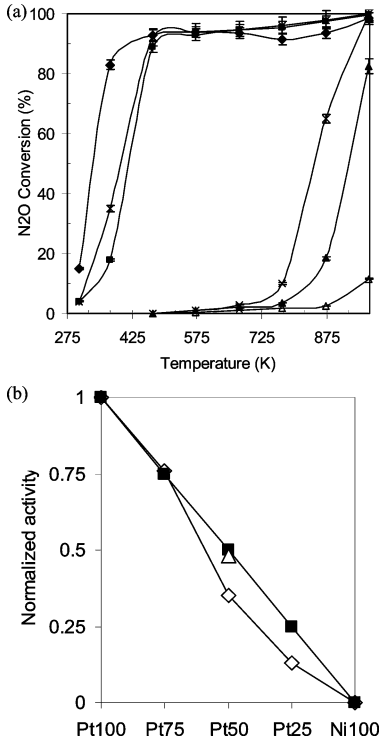

Figure 4. Catalytic performance of $Ni_{50}Pt_{50}$/S200. (a) Evolution of the N_2O conversion as a function of the reaction temperature for N_2O decomposition (D−M/SiO_2) and N_2O reduction by H_2 (R−M/SiO_2): ■, R−Ni+Pt/S200; ◆, R−$Ni_{50}Pt_{50}$/S200; △, D−Ni/S200; ▲, D−Ni_{50}-Pt_{50}/S200; ∗, R−Pt/S200; and ×, D−Pt/S200. (b) Normalized activity for N_2O decomposition at 773 K: ◇, Experimental activity; ■, Predicted activity; and △, Activity of a mechanical mixture Ni+Pt/S200 (Ni/Pt = 1).

atom or by direct reaction with another N_2O molecule. In these circumstances, the dissociative adsorption of N_2O on the surface of the catalysts leads to a progressive development of an oxygen layer that inhibits the adsorption and consequent reaction of more N_2O. In the presence of hydrogen, the reductant regenerates reduced active sites by removing the adsorbed oxygen atoms. The TPR experiments on calcined samples demonstrated (Figure 1) that the presence of Pt in the bimetallic catalysts contributes to facilitate the reduction of the nickel oxide, as shown by the shift of the reduction temperature of nickel oxide to lower temperature. On the other hand, the differences in catalytic reactivity displayed by the monometallic Ni and Pt catalysts suggest that the N_2O reaction could reveal information about the nature of the atoms present on the surface of the bimetallic particles.

Figure 4a shows the catalytic performance of the bimetallic $Ni_{50}Pt_{50}$ catalyst for N_2O decomposition (D−$Ni_{50}Pt_{50}$/S200) and for N_2O reduction by H_2 (R−$Ni_{50}Pt_{50}$/S200). The figure includes, for comparison purposes, the activity of a mechanical mixture of the monometallic Ni/SiO_2 and Pt/SiO_2 catalysts (Ni/Pt atomic ratio of 1 and denoted as R−Ni+Pt/S200) and that of the monometallic Pt/SiO_2 catalyst (D−Pt/S200 and R−Pt/S200). As observed, the activity of the $Ni_{50}Pt_{50}$ catalyst for decomposition of N_2O is lower compared to that of Pt. The same behavior was observed for the other bimetallic catalysts. Figure 4b shows, for the N_2O decomposition the normalized activity at 773 K, experimental and predicted behavior considering the nominal composition. The behavior of the mechanical mixture of the monometallic Ni/SiO_2 and Pt/SiO_2 catalysts (Ni/Pt atomic ratio of 1) is very close to the predicted activity value. This behavior is expected considering that in this catalyst Ni and Pt is present in the form of independent particles. The

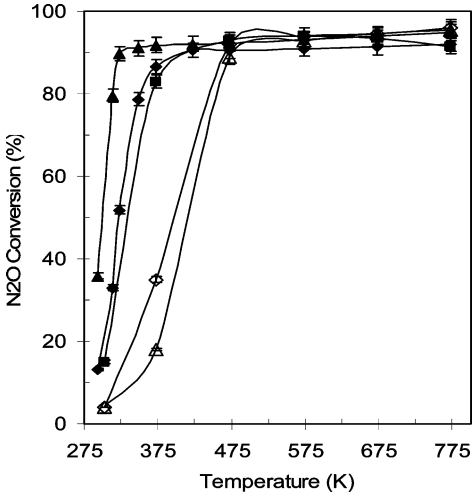

Figure 5. Performance of Ni−Pt/SiO_2 catalysts in N_2O reduction by hydrogen as a function of the reaction temperature: ■, $Ni_{50}Pt_{50}$/S200; ◆, $Ni_{25}Pt_{75}$/S200; ▲, $Ni_{75}Pt_{25}$/S200; △, Ni+Pt/S200; and ◇, Pt/S200.

activity observed for the $Ni_{25}Pt_{75}$ catalyst is also very close to the predicted value. For $Ni_{50}Pt_{50}$ and $Ni_{75}Pt_{25}$ samples, the N_2O conversion is lower than the one expected from additive catalytic properties. This result shows that the active surface of these bimetallic catalysts is composed of both active Pt atoms and less-active Ni atoms, leading to an ensemble size-sensitive behavior. The surface composition of bimetallic catalysts is often different from that in the bulk; additionally, surface enrichment in the presence of adsorbate gas molecules has been documented for bulk alloys and supported bimetallic systems. In particular, for the Ni−Pt system, Sedlacek et al.[33] reported that the surface of Pt−Ni alloys is enriched in Pt when the alloy is submitted to thermal treatments in H_2, while the inverse phenomenon is observed when the system is treated in O_2. For Ni−Pt catalysts, Wielers et al.[5] reported that surface enrichment in Ni is enhanced by oxidation. As mentioned previously, the dissociative adsorption of N_2O on the surface of the catalysts leads to a progressive development of an oxygen layer. Nickel enrichment in the surface promoted by this process could be possible and would explain why Ni−Pt alloys are less active for N_2O decomposition.

As in the case of monometallic catalysts, the addition of H_2 in the feed led to an increase of the reactivity of the samples. While, for the N_2O decomposition, the bimetallic catalyst is only active over 800 K, the presence of H_2 allows to one to achieve 50% N_2O conversion around 325 K. As observed, the bimetallic $Ni_{50}Pt_{50}$ catalyst (R−$Ni_{50}Pt_{50}$/S200) showed a better activity at lower temperature compared to the most active sample (R−Pt/S200). For this bimetallic catalyst, more than 80% of the N_2O is transformed at 350 K. At this temperature, Ni/S200 catalyst is practically inactive (Figure 3). On the other hand, the activity of the mechanical mixture (R−Ni+Pt/S200) is comparable to that observed for the Pt/SiO_2 catalyst.

Figure 5 shows the activity for the $N_2O + H_2$ reaction displayed by the bimetallic Ni−Pt/SiO_2 catalysts with a different Ni/Pt ratio. As observed, all bimetallic catalysts are very active at low temperature with the following activity order at 300 K: $Ni_{75}Pt_{25} > Ni_{25}Pt_{75} \approx Ni_{50}Pt_{50} >$ Pt/S200. As in the preceding reaction (N_2O decomposition), at low temperature the observed activity is due only to the Pt, since Ni was inactive (Figure 3). The turnover frequency (TOF) at 300 K is presented in Table 3. The total number of surface sites was estimated from particle size values determined by TEM (d_s), assuming that all metal particles are spheres of diameter d_s. Taking as reference the

TABLE 3: Turnover Frequency (TOF h^{-1}) at 300 K for the N_2O+H_2 Reaction

catalyst M/S200	TOF (h^{-1})
Pt	35
$Ni_{25}Pt_{25}$	88
$Ni_{50}Pt_{50}$	66
$Ni_{75}Pt_{25}$	169

M = Pt or Ni−Pt. S200 = SiO_2 Degussa.

TOF value for the Pt monometallic catalyst (35 h^{-1}), TOF values for the $Ni-Pt/SiO_2$ catalysts were about 2−5 times higher.

Infrared spectroscopy of adsorbed CO was used to get more information about the reactive surface in the bimetallic catalysts. Figure 6a displays the DRIFT spectra at room temperature of adsorbed CO on the surface of the $Ni-Pt/SiO_2$ catalysts. Frequencies in the range 2060−2090 cm^{-1}, which depend on the surface coverage and the reduction temperature, are attributed to linear (on top) CO adsorbed on Pt atoms.[34] On the other hand, CO forms with nickel linear Ni^0-CO species (band at ca. 2060−2025 cm^{-1}), $Ni-(CO)_x$ ($x = 2, 3$) subcarbonyls (ca. 2100−2070 cm^{-1}), bridged CO below 1800 cm^{-1}, and adsorbed $Ni(CO)_4$ (ca. 2150−2130, 2100−2030, and 2050−1830 cm^{-1}). Adsorption of CO on Pt/SiO_2 and Ni/SiO_2 monometallic samples produces broad bands with maxima at 2072 and 2077 cm^{-1}, respectively. The band at 2072 cm^{-1} is assigned to linear CO adsorbed on Pt atoms. The band at 2077 cm^{-1} is attributed to $Ni-(CO)_x$ subcarbonyls.[35] The IR spectra of CO adsorbed on the surface of the bimetallic catalysts are characterized by a single broad band. For $Ni_{50}Pt_{50}$ and $Ni_{25}Pt_{75}$ the maximum is at 2074 cm^{-1}, while for $Ni_{75}Pt_{25}$ the band is shifted to higher wavenumbers (ca. 2087 cm^{-1} with a shoulder at ca. 2066 cm^{-1}) with respect to what it is observed for Ni/SiO_2. In the spectral range 2066−2100 cm^{-1}, contributions of species adsorbed on both metals are included in the band making distinction between Pt and Ni surface atoms not evident. To determine if the absorption band observed in $Ni_{75}Pt_{25}$ catalyst could be due to CO adsorbed on Ni atoms, temperature was increased. The quantity of CO adsorbed irreversibly on Ni/SiO_2 decreases with increasing temperature.[36] Figure 6b shows the IR spectra collected at 423 K of preadsorbed CO at room temperature on Ni, Pt, and the bimetallic $Ni_{75}Pt_{25}$ catalysts. At this temperature the CO band was still observable for Pt/SiO_2; on the contrary, no band in the considered spectral region was observed for the Ni/SiO_2 catalyst. In view of this result, if CO adsorption on the surface of nominal Ni-rich bimetallic particles took place, at 423 K the band would practically disappear. The behavior of the CO band in the $Ni_{75}Pt_{25}$ bimetallic catalyst is similar to that observed for Pt. The band previously registered at room temperature remains but with lower intensity and shifted to lower wavenumbers, 2070 and 2082 cm^{-1} with a shoulder at 2057 cm^{-1} for Pt and $Ni_{75}Pt_{25}$, respectively. The same behavior of the CO band was observed for $Ni_{25}Pt_{75}$ and $Ni_{50}Pt_{50}$ catalysts (not shown).

The shift of the peak to lower wavenumbers with decreasing coverage is usually interpreted as resulting from decreasing coupling among oscillating adsorbed CO molecules. The coverage-dependent peak shift has also a chemical shift component. This is due to changes in the electron distribution between CO and the metal and can be either positive or negative.[37] Also, the heterogeneity of the surface may contribute to the observed peak shift. With the present results, it is not possible to separate these components in the IR spectra of the Ni−Pt catalysts. The high-frequency CO absorption band observed for the $Ni_{75}Pt_{25}$ (ca. 2082 cm^{-1} with a shoulder at ca. 2057 cm^{-1}) indicate linearly adsorbed CO on Pt sites of different coordination

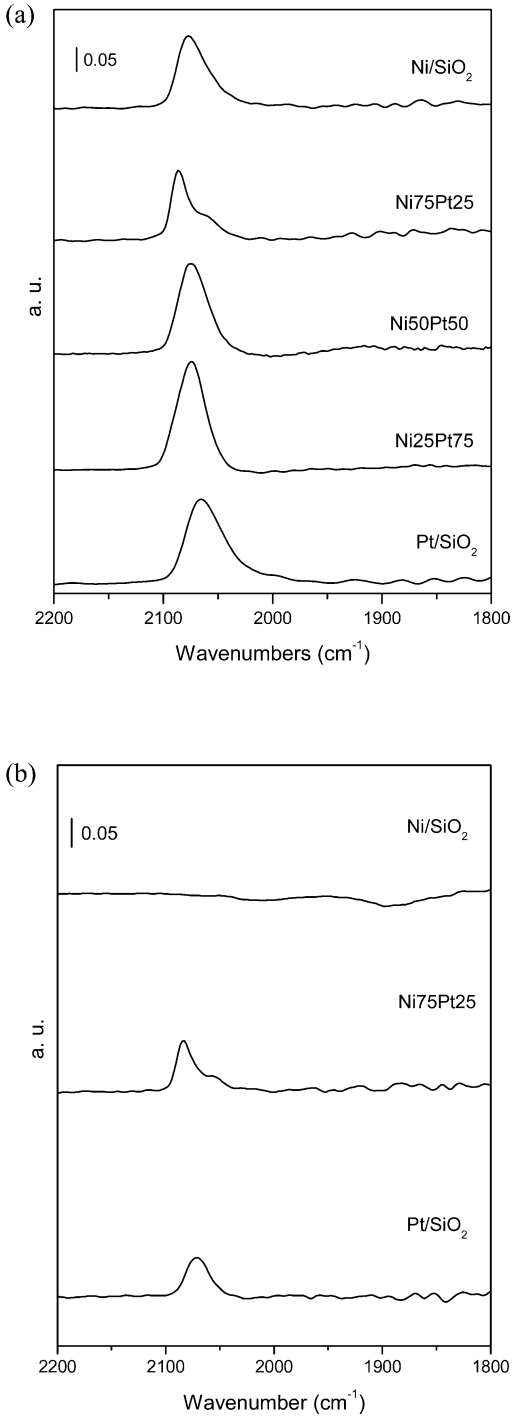

Figure 6. In situ DRIFT spectra of CO adsorbed at RT on $Ni-Pt/SiO_2$ catalysts and collected at (a) room temperature and (b) at 423 K.

number.[38−40] Qualitatively, CO adsorption characterized by DRIFT showed that the surfaces of the $Ni_{50}Pt_{50}$ and $Ni_{25}Pt_{75}$ catalysts seem similar to that of the monometallic Pt/S200 catalyst. On the contrary, the $Ni_{75}Pt_{25}$ catalyst showed a quite different behavior toward CO adsorption. The difference between the active surfaces in the bimetallic system is, on the other hand, demonstrated by the catalytic activity displayed by the bimetallic catalysts in the $N_2O + H_2$ reaction; while practically the same activity is observed for $Ni_{50}Pt_{50}$ and $Ni_{25}Pt_{75}$ catalysts, the TOF is higher for the $Ni_{75}Pt_{25}$ catalyst (Table 3). For $Ni_{75}Pt_{25}$ catalyst the enhanced activity as well as the observed CO absorption band indicate that Pt ensembles on the surface of this catalyst are different compared to Pt and

the bimetallic $Ni_{50}Pt_{50}$ and $Ni_{25}Pt_{75}$ catalysts. The catalytic behavior of bimetallic catalysts has been explained in terms of the ensemble effect (geometric effect) in which the average size and composition of the ensembles of active sites are varied due to the presence of the second metal and the electronic effect in which unexpected catalytic properties are the result of the modification of the electronic environment of the active phase due to alloying. The enhancement of the activity in the bimetallic $Ni-Pt/SiO_2$ catalysts could be explained in terms of an ensemble effect (small Pt clusters as Ni concentration increases). This explanation would easily rationalize the higher activity of the $Ni_{75}Pt_{25}$ sample; nevertheless, combined geometric and electronic effects (mixed ensembles) as proposed in the literature to explain the singular behavior of these alloy systems may not be excluded. The chemisorptive and catalytic properties of Ni_xPt_{1-x} alloys are different compared to the pure metals. $Ni_{50}Pt_{50}(111)$ and $Ni_{78}Pt_{22}(111)$ alloy surfaces that are Pt enriched present a weaker H_2 and CO adsorption compared to Pt(111) and Ni(111).[13] The same behavior is observed regarding the bond strength of unsaturated hydrocarbons with these surfaces. Moreover, the catalytic activity for 1,3-butadiene hydrogenation is notably enhanced on $Ni_{50}Pt_{50}(111)$. Cabeza et al.[41], using a semiempirical molecular orbital method, have shown that the binding energy of different molecules decreases significantly with respect to the pure metal surfaces, and they related this to electronic changes of the Pt states in the overlayer of Pt/Ni(111). Kitchin et al.[42] have recently shown, using DFT calculations to elucidate the origin of the weak metal−hydrogen bond on Ni/Pt(111) bimetallic surfaces, that subsurface Ni atoms modifies the electronic states of surface Pt atoms.

Theoretical calculations are in progress in order to obtain information about the electronic properties of bimetallic $Ni-Pt/SiO_2$ nanoparticles.

Conclusions

The surface properties of bimetallic $Ni-Pt/SiO_2$ catalysts with variable Ni/Ni + Pt atomic ratio (0.75, 0.50, and 0.25) were studied using N_2O decomposition and N_2O reduction by hydrogen reactions as probes. Mean particle size by TEM was in the range 6−8 nm for all catalysts and truly bimetallic particles (more than 95%) were evidenced by EDS in the $Ni-Pt/SiO_2$ catalysts. CO adsorption on the bimetallic catalysts showed differences in the linear CO absorption band as a function of the Ni/Pt atomic ratio.

For both model reactions, Pt/SiO_2 catalyst was substantially more active than Ni/SiO_2 catalyst. This suggests that N_2O as a probe could reveal information about the nature of the atoms present on the surface of bimetallic particles. Bimetallic $Ni-Pt/SiO_2$ catalysts showed, for the N_2O decomposition, a catalytic behavior that points to an ensemble-size sensitive behavior for Ni-rich compositions. No beneficial effects on the activity due to alloying were observed. For the $N_2O + H_2$ reaction, the following activity order at 300 K was observed: $Ni_{75}Pt_{25} > Ni_{25}Pt_{75} \approx Ni_{50}Pt_{50} >$ Pt. TOF values for bimetallic catalysts increased 2−5 times compared to the most active reference catalyst (Pt/SiO_2). The enhancement of activity in the bimetallic catalysts could be explained in terms of an ensemble effect (small Pt clusters as Ni concentration increases) but a combined geometric and electronic effect due to the presence of mixed ensembles to explain the catalytic behavior of these bimetallic systems may not be ruled out.

Acknowledgment. We thank Luis Rendón and Samuel Tehuacanero for technical assistance.

References and Notes

(1) Sinfelt, J. H. *Bimetallic Catalysts: Discoveries, Concepts and Applications*; John Wiley and Sons: New York, 1983.
(2) Ponec, V. *Appl. Catal., A* **2001**, *222*, 31.
(3) Ponec, V.; Bond, G. C. *Catalysis by Metals and Alloys*; Elsevier: Amsterdam, 1995; p 209.
(4) Dominguez, J. M.; Vazquez, A.; Renouprez, A. J.; Yacamán, M. J. *J. Catal.* **1982**, *75*, 101.
(5) Wielers, A.; Zwolsman, G.; Van der Grift, G.; Geus, J. W. *Appl. Catal.* **1985**, *19*, 187.
(6) Gauthier, Y.; Joly, Y.; Baudoing, R.; Rundgren, *J. Phys. Rev. B* **1985**, *31*, 6216.
(7) Gauthier, Y.; Baudoing, R.; Laundgren, M.; Rundgren, *J. Phys. Rev. B* **1987**, *35*, 7867.
(8) Gauthier, Y.; Baudoing, R.; Jupille, *J. Phys. Rev. B* **1987**, *40*, 1500.
(9) Weigand, P.; Jelinek, B.; Hofer, W.; Varga, P. *Surf. Sci.* **1994**, *301*, 306.
(10) Hebenstreit, W.; Ritz, G.; Schmid, M.; Biedermann, A.; Varga, P. *Surf. Sci.* **1997**, *388*, 150.
(11) Hofer, W. A.; Ritz, G.; Hebenstreit, W.; Schmid, M.; Varga, P.; Redinger, J.; Podloucky, R. *Surf. Sci.* **1998**, *405*, L514.
(12) Varga, P.; Schmid, M. *Appl. Surf. Sci.* **1999**, *141*, 287.
(13) Bertollini, J. C. *Appl. Catal., A* **2000**, *191*, 15.
(14) Raab, C.; Lercher, J. A.; Goodwin, J. G.; Shyu, J. Z. *J. Catal.* **1990**, *122*, 406.
(15) Oh, S. G.; Rodríguez N. M.; Baker, R. T. K. *J. Catal.* **1992**, *136*, 584.
(16) Englisch, M.; Vidyadhar; Radane, S.; Johannes, A. Lercher, *J. Mol. Catal. A* **1997**, 121, 69.
(17) Arai, M.; Ebina T.; Shirai, M. *Appl. Surf. Sci.* **1999**, *148*, 155.
(18) Aeiyach, S.; Garin, F.; Hilaire, L.; Legaré, P.; Maire, G. *J. Mol. Catal*. **1984**, *25*, 183.
(19) Massardier, J.; Tardy, B.; Abon, M.; Bertollini, J. C. *Surf. Sci.* **1983**, *126*, 154.
(20) Massardier, J.; Bertollini, J. C. *J. Catal.* **1984**, *90*, 358.
(21) Arenas-Alatorre, J.; Avalos-Borja, M.; Díaz, G. *Appl. Surf. Sci.* **2002**, *189*, 7.
(22) (a) Armor, J. *Appl. Catal. B* **1992**, *1*, 139. (b) Theimens, M. H.; Trogler, W. C. *Science* **1991**, *251*, 932.
(23) Granger, P.; Dathy, C.; Lecomte, J. J.; Leclercq, L.; Prigent, M.; Mabilon, G.; Leclercq, G. *J. Catal.* **1998**, *173*, 304.
(24) Kapteij, F.; Rodriguez-Mirasol, J.; Moulijn, J. A. *Appl. Catal., B* **1996**, *9*, 25.
(25) Avery, N. R. *Surf. Sci.* **1983**, *131*, 304.
(26) Hoffman, D. A.; Hudson, J. B. *Surf. Sci.* **1987**, *180*, 77.
(27) Sau, R.; Hudson, J. B. *J. Vac. Sci. Technol.* **1981**, *18*, 607.
(28) Orita, H.; Itoh, N. *Surf. Sci.* **2004**, *550*, 166.
(29) Redmond, J. P. *J. Phys. Chem.* **1993**, *67*, 267.
(30) Kim, M. H.; Ebner, J. R.; Friedman, R. M.; Vannice, M. A. *J. Catal.* **2001**, *204*, 348.
(31) Jentys, A.; MacHugh, B. J.; Haller, G.; Lercher, J. *J. Phys. Chem.* **1992**, *96*, 1324.
(32) Jentys, A.; Haller, G.; Lercher, J. *J. Phys. Chem.* **1993**, *97*, 484.
(33) Sedlacek, J.; Hilaire, L.; Legare, P.; Maire, G. *Surf. Sci*. **1982**, *115*, 541
(34) Davydov, A. A. In *Infrared Spectroscopy of Adsorbed Species on the Surface of Transition Metal Oxides*; Rochester, C. H., Ed.; John Wiley: 1984; p 101.
(35) Martra, G.; Swaan, H. M.; Mirodatos, C.; Kermarec, M.; Louis, C. *Stud. Surf. Sci. Catal.* **1997**, *111*, 617.
(36) Bartholomew, Y. C. H.; Pannell, R. B. *J. Catal.* **1980**, *65*, 390.
(37) Lauterbach, J.; Boyle, R. W.; Schick, M. Mitchell, W. J.; Meng, B.; Weinberg, W. H. *Surf. Sci.* **1996**, *350*, 32.
(38) Kim, H. M.; Ebner, R. J.; Friedman, M. R.; Vannice, A. M. *J. Catal.* **2001**, *204*, 348.
(39) Hopster, H.; Ibach, H. *Surf. Sci.* **1978**, *77*, 109.
(40) Greenler, R. G.; Burch, D. K.; Kretzschmar, K.; Klauser, R.; Bradshaw, A. M. *Surf. Sci.* **1985**, *152/153*, 338.
(41) Cabeza, G.F.; Castellani, N. J.; Legaré, P. *Comput. Mater. Sci.* **2000**, *17*, 255.
(42) Kitchin, R. J.; Khan, A. N.; Barteau, A. M.; Chen, G. J.; Yakshinskiy, B.; Madey, E. T. *Surf. Sci*. **2003**, *544*, 295.